100-LEVEL SMOOTHED SCINTISCANS PROCESSED AND PRODUCED BY A DIGITAL COMPUTER

W. Newlon Tauxe

Mayo Clinic and Mayo Foundation, Rochester, Minnesota

The advantages of handling scan data with digital computers have been documented (*1–7*). The use of data-filtering by the computer in conjunction with the collimator response characteristics has resulted in a superior representation of scan data which lets one represent easily up to 20 levels of activity on scans such as the one shown in Fig. 1. In this figure a conventional photoscan of a heart is shown with a computer-produced digital scan obtained from the same data.

A recent report by us (*8*) indicates that 20 levels may not always be enough. We based this conclusion on finding a small area of hepatic parenchymal nonfunction on one slice of a 20-level plot (confirmed to be neoplastic by needle biopsy at the site) which was not depicted clearly either on another 20-level plot of the same data in which the levels were slightly shifted or on a conventional photoscan.

This fact has prompted us to investigate the possibility of producing scans with more levels. Although 20-level plots do not trouble the eye in this scan format, individual plots containing more than 20 slices tend to become jumbled and distorted. Therefore we have placed an upper limit of 20 on the number of counting rates represented on the individual scan readout but have shifted these symbols over five slightly differing counting rates, resulting in a total of 100 levels. The purpose of this paper is to describe the method and to present examples of the scan formats.

METHOD

The basic method for data collection, storage and handling of computer-processed scans has been de-

Revision received April 11, 1967; accepted July 19, 1967.

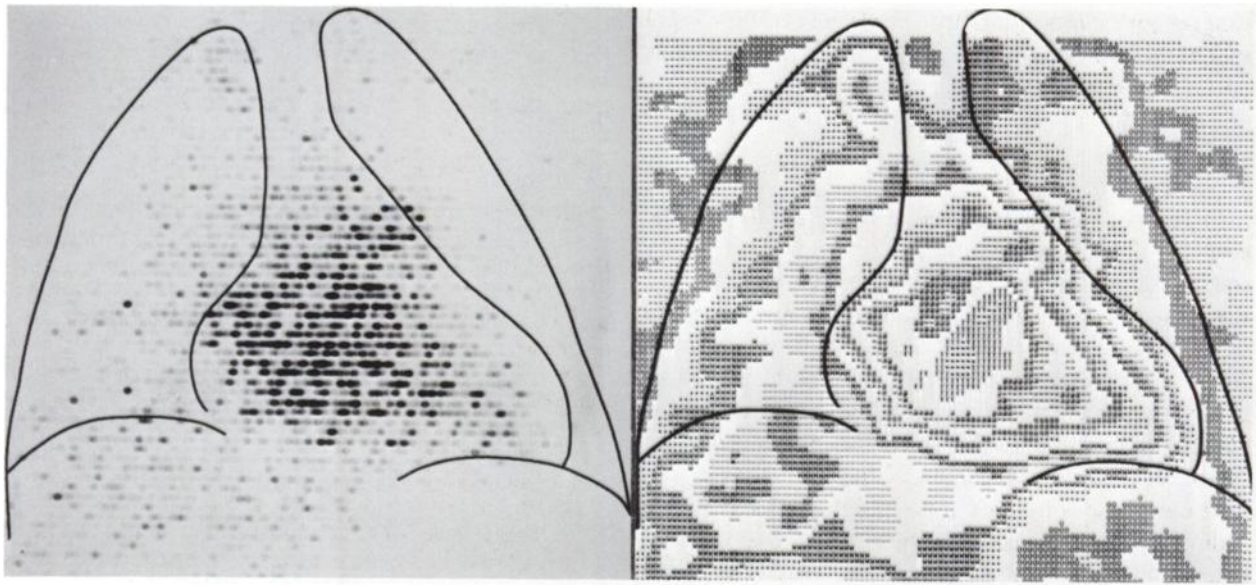

FIG. 1. Photoscan of heart (left) after injection of ^{131}I human serum albumin is registered against tracing made from parallax-free roentgenogram of chest. While most activity lies within heart shadow, no notion of counting rate is possible and little detail appears in extra-cardiac activity. In computer-processed digital plot of same scan matrix (right) much more anatomical detail is evident than in conventional photoscan at left. Carotid vessels are outlined by W's.

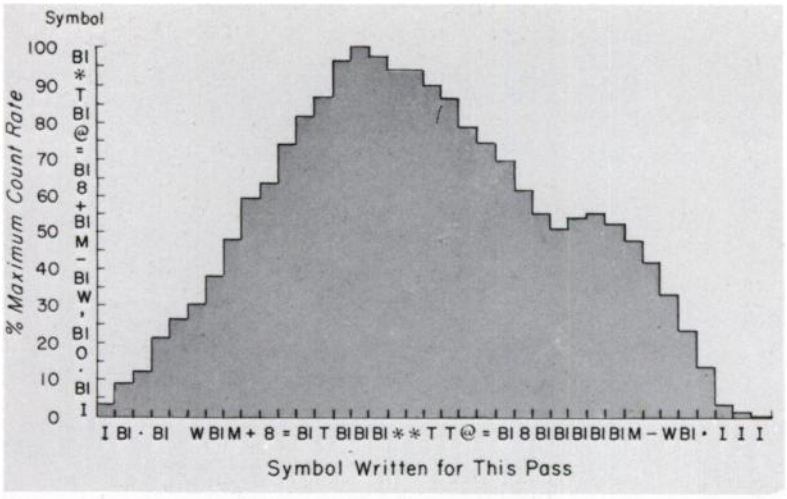

FIG. 2. Diagrammatic probe pass (above) containing maximum organ radioactivity shows individual units plotted as symbols representing 20 different intensity levels. Bl indicates Blank. See Table 1 for symbols.

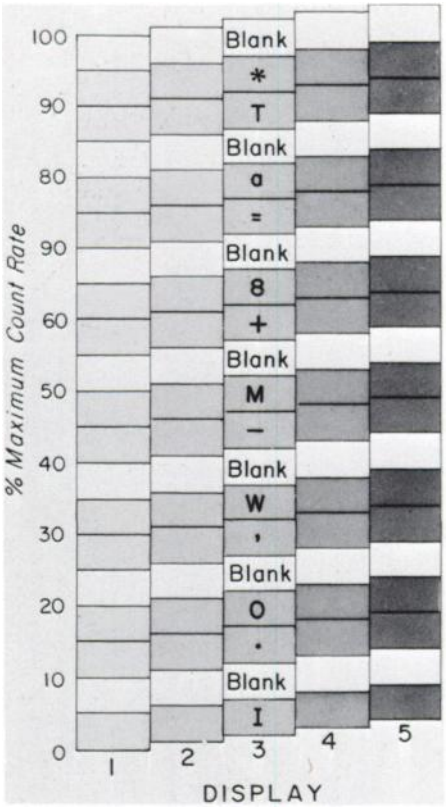

FIG. 3. Graph (at right) shows 100 counting increments in five plots of 20 levels each. Successive increments are given by same symbols.

scribed (*2,3,8,9*). Briefly, it involves collecting all the data contained on a radioisotope scan on an 8-channel digital-incremental tape recorder, processing it by a digital computer (IBM 7040) and reading it out by a high-speed (600 lines/min) typing device (IBM 1403 or Calcomp x-y plotter). The scans that are derived are compared with photoscans made in the conventional manner and registered against a tracing of the general anatomic landmarks derived from nonmagnifying roentgenograms made with the method of Lewall and Tauxe (*10*).

As reported previously, the computer is programmed to seek the highest counting rate on the digitized scan matrix (Fig. 2). It divides this peak value into 100 increments which are then programmed to be read out 20 at a time using a variety of symbols. Table 1 shows the symbols illustrating the 20 increments in this paper.

The computer is then programmed to shift the symbols to represent 20 different increments one fifth of the way between increments, to print these out and then to continue to shift the 20 increments successively by fifths until the 20 increments superimpose on themselves. This process is diagrammed in Fig. 3 where five separate shifted plots containing the symbols representing 20 different counting rates in constant increments are represented by 100 different counting levels. These can be represented singly, or a representation can be made on a single readout by superimposing the prints in registry.

The digitized scans in this paper were derived from scans of patients sent for routine scanning procedures, and they include those of liver, lung, heart, brain and thyroid.

TABLE 1. SYMBOLS FOR COUNTING-RATE LEVELS

Level	Symbol	Level	Symbol
1	I	11	Blank
2	Blank	12	+
3	.	13	8
4	0	14	Blank
5	Blank	15	=
6	,	16	@
7	W	17	Blank
8	Blank	18	T
9	—	19	*
10	M	20	Blank

RESULTS

Figure 4A shows the anteroposterior lung photoscan of a normal subject following injection in the upright position of 200 μc of ^{131}I-labeled macroaggregated albumin. The tracing of pertinent landmarks made from a nonmagnifying roentgenogram is superimposed on scan. Figure 4B–F shows the 100 levels separately. Actual counting rates and symbols as-

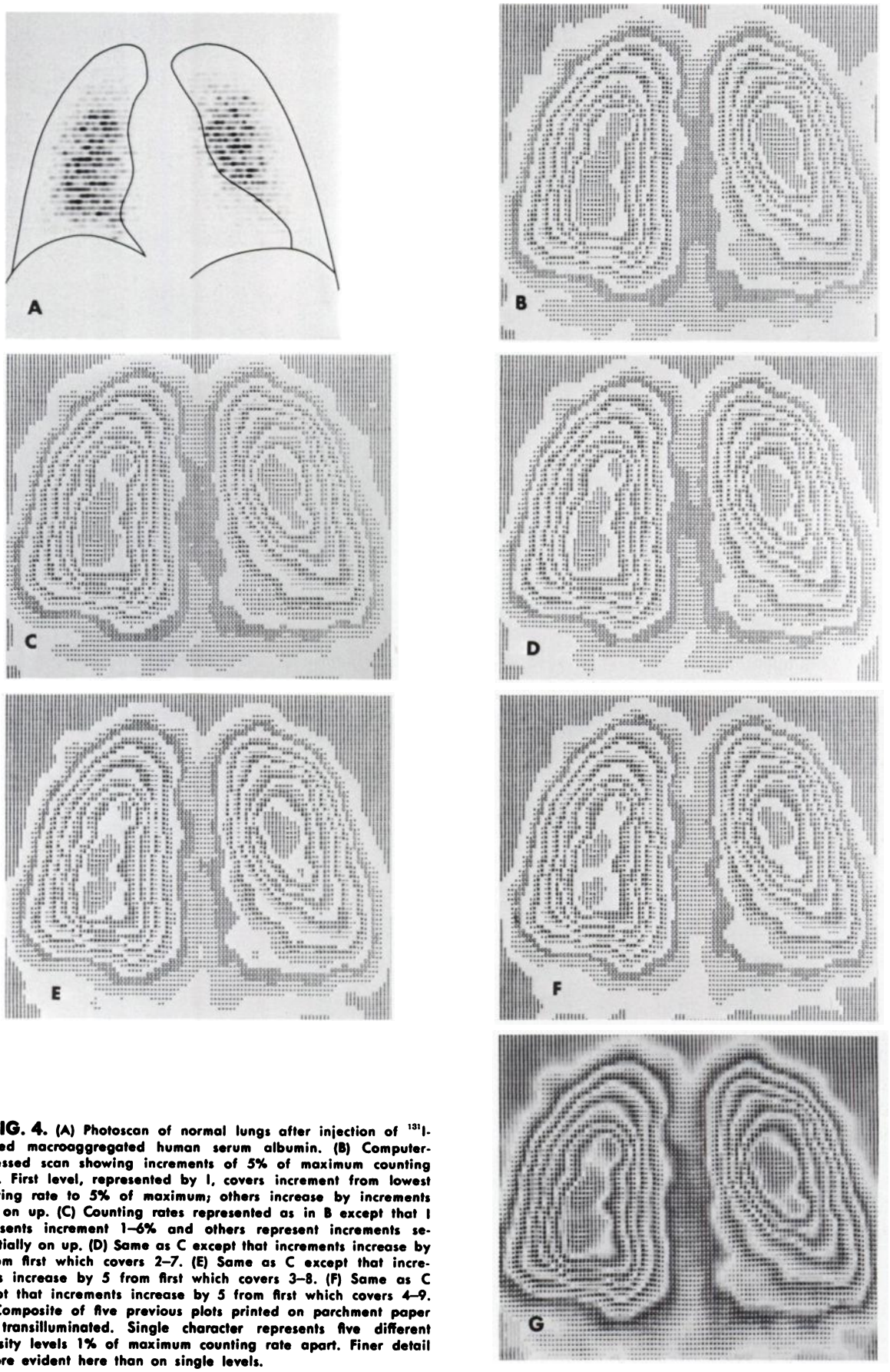

FIG. 4. (A) Photoscan of normal lungs after injection of ^{131}I-labeled macroaggregated human serum albumin. (B) Computer-processed scan showing increments of 5% of maximum counting rates. First level, represented by I, covers increment from lowest counting rate to 5% of maximum; others increase by increments of 5 on up. (C) Counting rates represented as in B except that I represents increment 1–6% and others represent increments sequentially on up. (D) Same as C except that increments increase by 5 from first which covers 2–7. (E) Same as C except that increments increase by 5 from first which covers 3–8. (F) Same as C except that increments increase by 5 from first which covers 4–9. (G) Composite of five previous plots printed on parchment paper and transilluminated. Single character represents five different intensity levels 1% of maximum counting rate apart. Finer detail is more evident here than on single levels.

signed to represent them are given in Table 2. Figure 4G at the foot of the page is a transilluminated superposition of the five levels in order and in registry. These levels are printed on parchment paper* for transillumination.

Figure 5 is a 100-level composite scan of the heart of a patient referred because of a question of intracardiac tumor (see Fig. 1). In this case no tumor was found, but details of the radioactivity distribution are much more evident than they are on other forms of data presentation. For example, quasi-structured areas peripheral to the heart are clearly shown by the computer-processed multilevel scan—probably better than they are on the photoscan.

Figure 6 is the composite of a similar liver series in a patient with biliary cirrhosis. Figure 7 is a scan of a brain, and Fig. 8 is a scan of a thyroid.

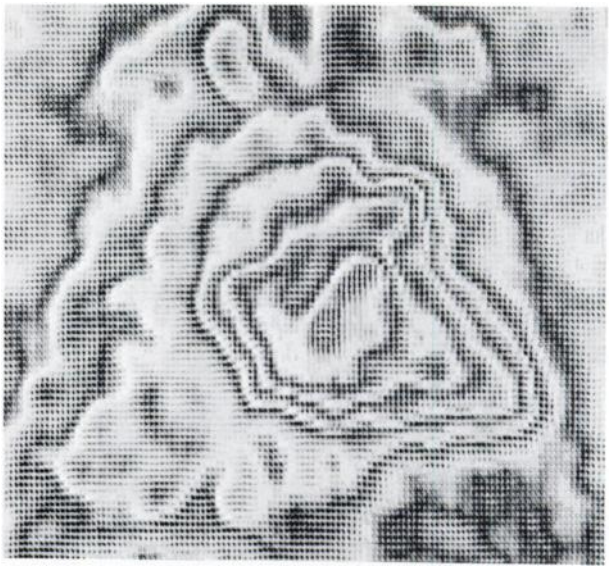

FIG. 5. 100-level plot of heart scan in Fig. 1. More detail is shown here than in photoscan or in single scan in which only 20 levels are depicted. To produce sensation of height in smooth transition from bottom to top, one can imagine that one is looking at layered cake.

DISCUSSION

In our preliminary investigation, scans of the type described here seemed to have their most important application in the area of the lung, liver, thyroid, brain, heart and spleen.

Work is now underway to determine the optimal percentage levels for routine clinical use. Scan information in all the forms described here—equal 100 levels superimposed or separated as five 20-level plots—is available from the data presentations described. All of these can be carried out easily and inexpensively on a digital computer and stored on a small length of magnetic tape.

* Moore Business Form Company, Niagara Falls, N.Y. (16-lb. White Roadmaster parchment #216, 14⅞ X 11 in.)

TABLE 2. COUNTING RATES AND SYMBOLS FOR LUNG SCANS IN FIG. 4

Counting rates (cpm) for:					Symbol
Fig. 4B	Fig. 4C	Fig. 4D	Fig. 4E	Fig. 4F	
0– 317	63– 380	127– 443	190– 507	253– 570	I
317– 633	380– 697	443– 760	507– 823	570– 887	Blank
633– 950	697–1,013	760–1,077	823–1,140	887–1,203	.
950–1,267	1,013–1,330	1,077–1,393	1,140–1,457	1,203–1,520	0
1,267–1,583	1,330–1,647	1,393–1,710	1,457–1,773	1,520–1,837	Blank
1,583–1,900	1,647–1,963	1,710–2,027	1,773–2,090	1,837–2,153	,
1,900–2,217	1,963–2,280	2,027–2,343	2,090–2,407	2,153–2,470	W
2,217–2,533	2,280–2,597	2,343–2,660	2,407–2,723	2,470–2,787	Blank
2,533–2,850	2,597–2,914	2,660–2,977	2,723–3,040	2,787–3,104	–
2,850–3,167	2,914–3,230	2,977–3,294	3,040–3,357	3,104–3,420	M
3,167–3,484	3,230–3,547	3,294–3,610	3,357–3,674	3,420–3,737	Blank
3,484–3,800	3,547–3,864	3,610–3,927	3,674–3,990	3,737–4,054	+
3,800–4,117	3,864–4,180	3,927–4,244	3,990–4,307	4,054–4,370	8
4,117–4,434	4,180–4,497	4,244–4,560	4,307–4,624	4,370–4,687	Blank
4,434–4,750	4,497–4,814	4,560–4,877	4,624–4,940	4,687–5,004	=
4,750–5,067	4,814–5,130	4,877–5,194	4,940–5,257	5,004–5,320	@
5,067–5,384	5,130–5,447	5,194–5,510	5,257–5,574	5,320–5,637	Blank
5,384–5,700	5,447–5,764	5,510–5,827	5,574–5,890	5,637–5,954	T
5,700–6,017	5,764–6,080	5,827–6,144	5,890–6,207	5,954–6,270	*
6,017–6,334	6,080–6,397	6,144–6,460	6,207–6,524	6,270–6,587	Blank

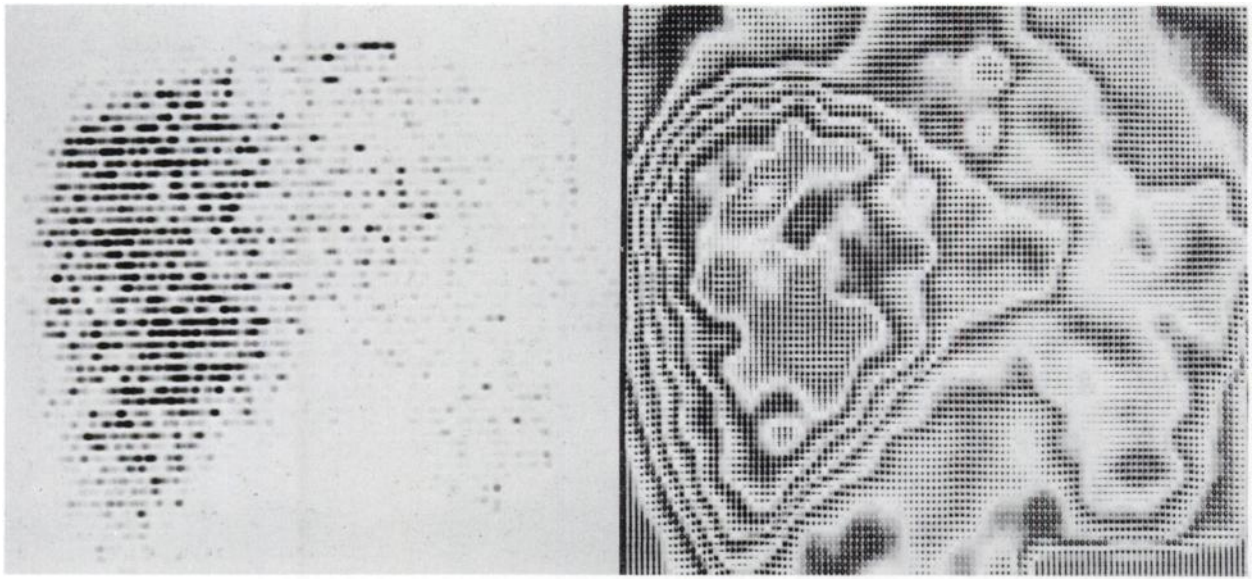

FIG. 6. Scan of liver in patient with biliary-cirrhosis following injection of rose bengal ^{131}I. Photoscan (left) shows generalized mottling which might indicate either low counting rate or presence of regenerative nodules. Computer-processed plot (right) shows distinct nodular pattern to central portions of liver, smooth edges where counting rates are lower and radioactivity still in blood in heart, spleen and kidney. Patterns can not be clearly discerned in photoscan.

SUMMARY

A method of computer handling scintiscan matrices affording 100 levels of digitized counting-rate intensity is described which promises great clinical usefulness with advantages of speed, high resolution, accuracy and low cost.

REFERENCES

1. BROWN, D. W.: Digital computer analysis and display of the radioisotope scan. *J. Nucl. Med.* **5**:802, 1964.

2. TAUXE, W. N. AND CHAAPEL, D. W.: Contrast-enchantment of scanning procedures by high-speed computer (abstr). *J. Nucl. Med.* **6**:326, 1965.

3. TAUXE, W. N., BURCHELL, H. B., CHAAPEL, D. W. AND SPRAU, A. C.: Quantitating the effect of gravity on lung scans of macroaggregates of albumin-^{131}I. *J. Appl. Physiol.* **21**:1,381, 1966.

4. SCHEPERS, H. AND WINKLER, C.: An automatic scanning system using a tape perforator and computer techniques. In *Medical radioisotope scanning*. IAEA, Vienna, 1964, 321.

5. KENNY, P. J., LAUGHLIN, J. S., WEBER, D. A., COREY, K. R. AND GREENBERG, E.: High-energy gamma-ray scanner. In *Progress in medical radioisotope scanning* (TID 7673), USAEC, Washington, D.C., 1963, 236.

6. BENDER, M. A. AND BLAU, M.: Autofluoroscopy: The use of a non-scanning device for tumor localization with radioisotopes (abstr). *J. Nucl. Med.* **1**:105, 1960.

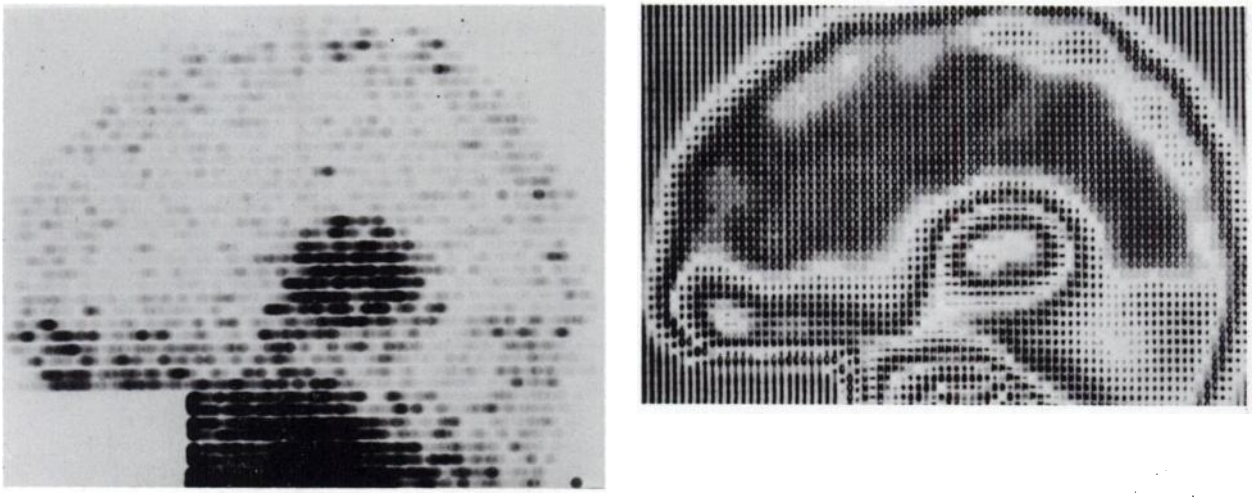

FIG. 7. Brain scan of patient with astrocytoma grade 3 following injection of ^{99m}Tc pertechnetate. Photoscan (left) shows tumor clearly. However, area around tumor is mottled, and little anatomical detail is evident. Computer-processed scan (right) reveals information given in scan but also delineates anatomical details of head clearly.

7. COREY, K. R. AND BENUA, R. S.: Progress in radioactive isotope scanning. *Med. Clin. N. Am.* **50**:689, 1966.

8. SPRAU, A. C., TAUXE, W. N. AND CHAAPEL, D. W.: Computerized radioisotope-scan-data filter based on system response to point source. *Mayo Clin. Proc.* **41**:585, 1966.

9. TAUXE, W. N.: Digital computer processing of radioisotope scintiscan matrices. Submitted for publication.

10. LEWALL, D. B. AND TAUXE, W. N.: A method for the elimination of magnification in roentgenograms for scintiscan superimposition. *Am. J. Clin. Path.* In press.

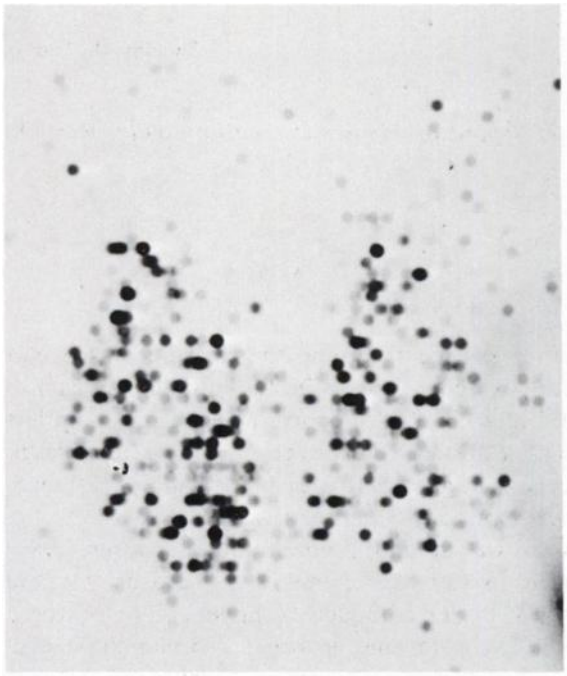

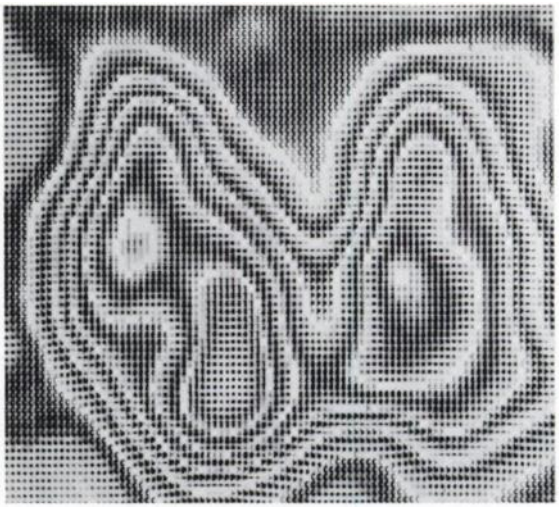

FIG. 8. Thyroid photoscan (left), made after patient was given regular tracer oral dose of 5 μc ^{131}I, is virtually uninterpretable. Only 0.8 μc ^{131}I was in thyroid at time of scan. In 100-level digital scan (above) relatively hot nodule is seen in inferior pole of right lobe. Scan shows ability of computer to handle very low counting rates well.